

Supplementary material

Insight into the Mechanism About the Initiation, Growth and Termination of C–C Chain in Syngas Conversion on Co(0001) Surface: A Theoretical Study

Guangxiang Wen,^a Qiang Wang,^b Riguang Zhang,^{a,*} Debao Li,^b Baojun Wang,^{a,*}

^a Key Laboratory of Coal Science and Technology of Ministry of Education and Shanxi Province, Taiyuan University of Technology, Taiyuan 030024, Shanxi, P.R. China

^b State Key Laboratory of Coal Conversion, Institute of Coal Chemistry, Chinese Academy of Science, Taiyuan 030001, Shanxi, PR China

Part 1. The Standard Molar Gibbs Free Energy for Gaseous Species and Adsorbed Species

The standard molar Gibbs free energy are calculated according to below Eq. (1):

$$G^\theta(T, p) = E_{total} + E_{ZPE} + U^\theta - TS^\theta + \gamma RT \left[1 + \ln(p_{CO}/p^\theta) \right] \quad (1)$$

For surface reactions, only vibration modes were taken into account. All the vibrational frequencies ν_i (Hz) were calculated based on the statistical mechanics.¹⁻⁴ E_{ZPE} is the zero-point vibration energy, which is calculated by Eq. (2):

$$E_{ZPE} = \sum_{i=1} \frac{h\nu_i}{2} \quad (2)$$

Here h is Planck's constant and ν_i is the vibrational frequency.

U_{vib}^θ is the standard molar vibrational thermal energy, which is calculated by Eq. (3):

$$U_{vib}^\theta = R \sum_{i=1} \frac{h\nu_i/k_B}{e^{h\nu_i/k_B T} - 1} \quad (3)$$

* Corresponding author at: No. 79 Yingze West Street, Taiyuan 030024, China. Tel.: +86 351 6018239; Fax: +86 351 6041237 E-mail address: zhangriguang@tyut.edu.cn (Riguang Zhang); wangbaojun@tyut.edu.cn; quantumtyut@126.com (Baojun Wang)

where k_B is Boltzmann's constant, R is the gas constant.

The standard molar vibrational entropy is calculated using the following Eq. (4):

$$S_{vib}^{\theta} = \sum_{i=1}^n \left[-R \ln(1 - e^{-h\nu_i/k_B T}) + \frac{N_A h \nu_i}{e^{h\nu_i/k_B T} - 1} \frac{1}{T} \right] \quad (4)$$

where R is the gas constant.

The relationship between molar enthalpy and the thermal energy is given by Eq. (5):

$$H^{\theta} = U^{\theta} + \gamma RT \quad (5)$$

γ is 0 for surface CO adsorbed species, and 1 for gaseous CO molecule.

In the adsorption/desorption steps, as for the adsorbed species, although the translational and rotational modes are frustrated movements, the translational, rotational contributions are also taken into account for gaseous species. For a gas molecule moving in the three-dimensional (3D) space, the standard molar translational internal energy is given by Eq. (6):

$$U_{trans-3D}^{\circ} = \frac{3}{2} RT \quad (6)$$

The standard molar translational entropy follows Eq. (7):³

$$S_{trans-3D}^{\circ} = R \left[\ln \left(\frac{(2\pi m k_B T)^{3/2}}{h^3} \right) + \ln \left(\frac{V}{N_g} \right) + \frac{5}{2} \right] \quad (7)$$

where m is the mass of the molecule and V/N_g is the volume per molecule in the standard state. For a nonlinear molecule, the standard molar rotational internal energy contribution is obtained by Eq. (8):

$$U_{rot}^{\circ} = \frac{3}{2} RT \quad (8)$$

The standard molar rotational entropy contribution is obtained by the equation (9):

$$S_{rot}^{\circ} = R \left[\ln \left(\frac{8\pi^2 \sqrt{8\pi^3 I_x I_y I_z} (k_B T)^{3/2}}{\sigma h^3} \right) + \frac{3}{2} \right] \quad (9)$$

where I_x , I_y , and I_z are the three moments of inertia about the principal axes and σ is the rotational symmetry number.

Part 2. H₂ Adsorption and Dissociation, and its Existence Form on Co(0001) Surface

For H₂ adsorption on Co(0001) surface, two adsorption modes have been considered, one is the parallel mode, the other is the vertical mode.

For H₂ adsorption with the parallel mode, it is found that H₂ molecule prefers to adsorb at the top site with two H atoms bonding with one Co atom, the H–Co bond length is 1.62 Å, and the H–H bond is obviously elongated to 0.90 Å compared to 0.75 Å in gas phase, as shown in Figure S1(a), the corresponding adsorption energy is -30.8 kJ·mol⁻¹, indicating that the adsorption can contribute to the H–H bond activation of H₂, which is in favor of H₂ dissociation; meanwhile, H₂ adsorbed initially at the bridge site is also converted into the top site adsorption after geometry optimization. However, H₂ adsorptions with the parallel mode at the fcc and hcp sites are the dissociative adsorption, in which H₂ molecule is dissociated into two H atoms adsorbed on Co(0001) surface.

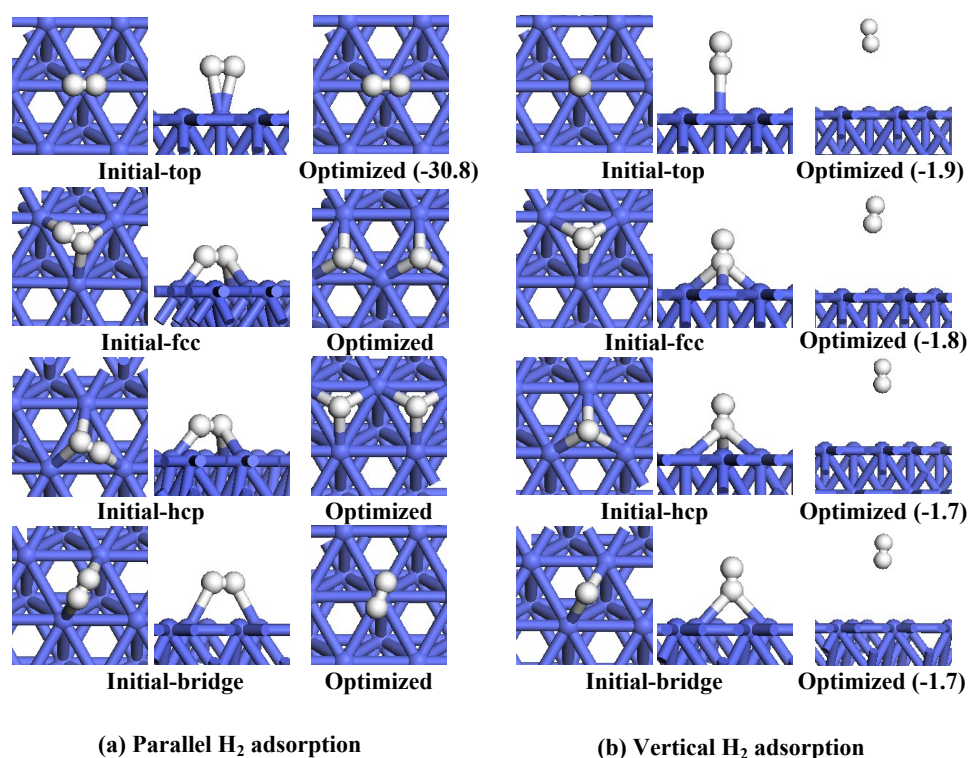


Figure S1 The optimized configurations of the single H₂ adsorption with the parallel and vertical modes on Co(0001) surface. Co and H atoms are shown in the purple and white balls, respectively. The unit is in kJ·mol⁻¹.

In the case of H₂ adsorption with the vertical mode, the optimized configurations show that H₂ molecules initially adsorbed at the bridge, fcc, hcp and top sites are all far away from the surface, which have the very weak adsorption energies of -1.8, -1.8, -1.7 and -1.9 kJ·mol⁻¹, as shown in [Figure S1\(b\)](#), the H–H bond length is hardly changed with respect to that for the free H₂ molecule.

Thus, for H₂ adsorption, H₂ adsorption with the parallel mode at the fcc and hcp sites over Co(0001) surface are dominantly focused on the dissociative adsorption; only the single H₂ adsorption with the parallel mode at the top site is the most stable configuration of molecule adsorption. However, the other adsorption configurations are not favored over Co(0001) surface.

For the dissociation of H₂ adsorption with the parallel mode at the top site, this elementary reaction is exothermic 73.2 kJ·mol⁻¹ with only an activation barrier of 8.0 kJ·mol⁻¹, which is rather low compared to its desorption energy (31.0 kJ·mol⁻¹), indicating that H₂ dissociation is favorable both kinetically and thermodynamically rather than its desorption.

Part 3. Adsorptions of all Possible Species

The adsorption of all possible species involved in syngas conversion over four adsorption sites of Co(0001) have been examined, and the most stable adsorption configurations are displayed in [Figure S2](#) in the main text; the corresponding adsorption free energies at 500 K, as well as the key structural parameters are listed in [Table S1](#).

C, H and O C and O prefer to adsorb at the hcp site, while H prefers to adsorb at the fcc site, which agree with the previous DFT results.^{5,6} The adsorption free energies of C, H and O atoms are 657.5, 247.7 and 570.2 kJ·mol⁻¹, respectively.

CO and OH CO and OH species prefer to adsorb at the hcp site, where CO adsorbed via C atom with the C–O bond perpendicular to the surface, which agrees with the previous DFT results,³ the adsorption free energy is 115.6 kJ·mol⁻¹. OH adsorbs via its O atom with its O–H bond

perpendicularly, the adsorption free energy is 299.8 kJ·mol⁻¹.

CH, CH₂ and CH₃ CH and CH₂ species prefer to adsorb at the hcp site via C atoms, while CH₂ is asymmetrically adsorbed at the hcp site, which agree with the results obtained by Ge *et al.*⁷ CH₃ prefers to adsorb at the fcc site via C atom. The adsorption free energies of CH, CH₂ and CH₃ are 565.9, 336.5 and 143.2 kJ·mol⁻¹, respectively.

CHO, CH₂O and CH₃O CHO, CH₂O and CH₃O species all prefer to adsorb at the hcp site. CHO binds to the surface with the bridge(O)-bridge(C) configuration, the adsorption free energy is 171.3 kJ·mol⁻¹. CH₂O prefers to the top(C)-hcp(O) configuration, the adsorption free energy is 37.3 kJ·mol⁻¹. CH₃O prefers to adsorb through its O atom with the O–C bond perpendicular to the surface, the adsorption free energy is 230.3 kJ·mol⁻¹.

COH, CHOH and CH₂OH COH and CHOH species prefer to adsorb at the hcp site via their C atoms, in which COH adsorbed with the C–O bond perpendicular to the surface, while CHOH adsorbs with the O–H bond pointing toward the surface, which well agrees with the previous studies by Cheng *et al.*,⁸ the adsorption free energies of COH and CHOH species are 375.5 and 249.4 kJ·mol⁻¹, respectively. CH₂OH adsorbs at the bridge site via both C and O atoms with an adsorption free energy of 110.9 kJ·mol⁻¹, in which the C–O bond is almost parallel to the surface.

CH₄, CH₃OH and H₂O CH₄, CH₃OH and H₂O species are all weakly bound to Co(0001) surface, the optimized structure of CH₄ is away from the surface with only an adsorption free energy of -1.8 kJ·mol⁻¹, which means that CH₄ is far away from the surface. Both CH₃OH and H₂O species prefer to adsorb at the top site via the O atom, in which the plane of adsorbed H₂O is nearly parallel to the surface, the adsorption free energies of CH₃OH and H₂O are 4.1 and -1.2 kJ·mol⁻¹, respectively.

Table S1 Adsorption free energies (G_{ads}) at 500 K, as well as the corresponding key structural parameters of the stable configurations for the adsorbed species involving in syngas conversion on Co(0001) surface.

Species	$G_{\text{ads}}(\text{kJ}\cdot\text{mol}^{-1})^*$	Adsorption/configuration	$D_{\text{Co-X}}(\text{\AA})$	Bonding details	
				bond	length (\AA)
C	657.5(674.6)	hcp: through C	1.78	—	—
H	247.7(255.7)	fcc: through H	1.74	—	—
O	570.2(581.9)	hcp: through O	1.8	—	—
CO	115.6(165.5)	hcp: through C	1.97	C-O	1.20
OH	299.8(350.9)	hcp: through O	2.00	O-H	0.97
CH	565.9(615.1)	hcp: through C	1.86	C-H	1.10
CH ₂	336.5(394.4)	hcp: through C	1.95/1.95/1.97	C-H	1.10/1.17
CH ₃	143.2(195.8)	fcc: through C	2.15/2.15/2.15	C-H	1.12
CHO	171.3(215.4)	hcp: C-bridge, O-bridge	1.86/2.07, 2.03/2.11	C-O/C-H	1.33/1.11
CH ₂ O	37.3(79.2)	hcp: C-top, O-hcp	1.98, 2.13/2.03/2.04	C-O/C-H	1.38/1.10
CH ₃ O	230.3(264.3)	hcp: through O	2.00	C-O/C-H	1.44/1.10
COH	375.5(415.7)	hcp: through C	1.87/1.89/1.90	C-O/O-H	1.34/0.98
CHOH	249.4(289.2)	hcp: through C	1.97/1.96/1.96	C-H/C-O/O-H	1.22/1.38/0.98
CH ₂ OH	110.9(147.6)	bridge: C-top, O-top	1.99, 2.15	C-H/C-O/O-H	1.10/1.47/0.98
CH ₄	-1.8(3.4)	away from the surface	—	C-H	1.10
CH ₃ OH	4.1(30.5)	top: through O	2.20	C-H/C-O/O-H	1.10/1.45/0.98
H ₂ O	-1.2(27.7)	top: through O	2.23	O-H	0.98
C ₂ H ₂	227.7(254.1)	α -C-fcc, β -C-hcp	2.03, 2.04	C-C	1.40
C ₂ H ₄	44.9(83.0)	α -C-hcp, β -C-top	2.26/2.25/2.10, 2.01	C-C	1.45
C ₂ H ₆	0.6(5.3)	away from the surface	—	C-C	1.53
CHCO	292.9(334.6)	α -C-fcc, β -C-hcp	2.06/2.06	C-O/C-H	1.10/1.26
CH ₂ CO	64.2(99.3)	fcc: α -C-top, β -C-bridge	1.87/2.00/2.1	C-O/C-C	1.34/1.43
CH ₃ CO	166.9(203.9)	hcp: α -C-top, O-bridge	1.83/2.09/2.11	C-O	1.31
CHCHO	380.3(420.8)	β -C-hcp, O-top	2.12/2.07/1.98, 1.97	C-C/C-O	1.42/1.29
CH ₂ CHO	179.5(205.7)	β -C-top, O-top	2.07, 1.92	C-O/C-C	1.32/1.43
CH ₃ CHO	14.3(30.9)	top: through O	2.09	C-O/C-C	1.24/1.49
CH ₃ CH ₂ O	182.1(196.1)	top: through O	1.81	C-O/C-C	1.42/1.52
C ₂ H ₅ OH	15.6(32.4)	top: through O	2.19	C-O/C-C	1.46/1.51
CH ₂ CH	228.6(276.8)	hcp: α -C-hcp, β -C-top	1.93/2.02/2.00, 2.11	C-C	1.42
CH ₃ CH	342.2(353.8)	fcc: through α -C	1.96/1.96/2.01	C-C	1.52
CH ₃ CH ₂	113.2(154.4)	fcc: through α -C	2.14/2.19/2.21	C-C	1.54
CH ₃ CHCH	236.0(279.6)	hcp: α -C-top, β -C-hcp	2.04/2.01/2.01	C-C-C	1.42/1.51
CH ₃ CHCH ₂	39.9(70.9)	hcp: α -C-top, β -C-hcp	2.27/2.21/2.10	C-C-C	1.45/1.51
CH ₃ CHCHO	156.5(191.4)	fcc: O-bridge, C-top	2.05/2.05, 2.08	C-C-C/C-O	1.43/1.52, 1.36
CH ₃ CH ₂ CHO	-5.4(24.2)	bridge: through O	2.13/2.06	C-C-C/C-O	1.48/1.53, 1.26
CH ₃ CH ₂ CHCHO	178.9(211.0)	fcc: O-bridge, C-top	2.07/2.05, 2.08	C-C-C-C/C-O	1.53/1.52/1.43, 1.36

* It is noted that the values in the parentheses is the adsorption free energies at 0 K.

C₂H₂, C₂H₄ and C₂H₆ C₂H₂ prefers to adsorb on the surface with one C atom placed at the fcc site, while the other C atom placed at the hcp site, the adsorption free energy is 227.7 kJ·mol⁻¹. C₂H₄ adsorbs with a hcp(C)-top(C) configuration, the adsorption free energy is 44.9 kJ·mol⁻¹. While C₂H₆ is away from the surface with only an adsorption free energy of 0.6 kJ·mol⁻¹.

CHCO, CH₂CO and CH₃CO CHCO prefers to adsorb with one C atom at the fcc site while the other C atom at the adjacent hcp site, the adsorption free energy is 292.9 kJ·mol⁻¹. CH₂CO prefers to adsorb at the fcc site with the bridge(C)-top(C) configuration, the adsorption free energy is 64.2 kJ·mol⁻¹. CH₃CO prefers to adsorb at the bridge(O)-top(α -C) configuration with an adsorption free energy of 166.9 kJ·mol⁻¹.

CHCHO, CH₂CHO and CH₃CHO CHCHO prefers to the hcp(β -C)-top(O) configuration with an adsorption free energy of 380.3 kJ·mol⁻¹. CH₂CHO prefers to the top(β -C)-top(O) configuration with an adsorption free energy of 179.5 kJ·mol⁻¹. CH₃CHO adsorbs at the top site via O atom with an adsorption free energy of 24.3 kJ·mol⁻¹.

CH₃CH₂O and C₂H₅OH CH₃CH₂O prefers to the top site via O atom with the adsorption free energy of 182.1 kJ·mol⁻¹. C₂H₅OH is also adsorbed at the top site via O atom with the adsorption free energy of 15.6 kJ·mol⁻¹.

CH₂CH, CH₃CH and CH₃CH₂ CH₂CH adsorbed via α -C atom placed at the hcp site while the β -C atom placed at the top site, the adsorption free energy is 228.6 kJ·mol⁻¹. CH₃CH and CH₃CH₂ prefer to adsorb at the fcc site via the α -C atom, the adsorption free energies are 342.2 and 113.2 kJ·mol⁻¹, respectively.

CH₃CHCH and CH₃CHCH₂ Both CH₃CHCH and CH₃CHCH₂ prefer to adsorb at the hcp site with the top(α -C)-hcp(β -C) configuration, the corresponding adsorption free energies are 236.0 and 39.9 kJ·mol⁻¹, respectively.

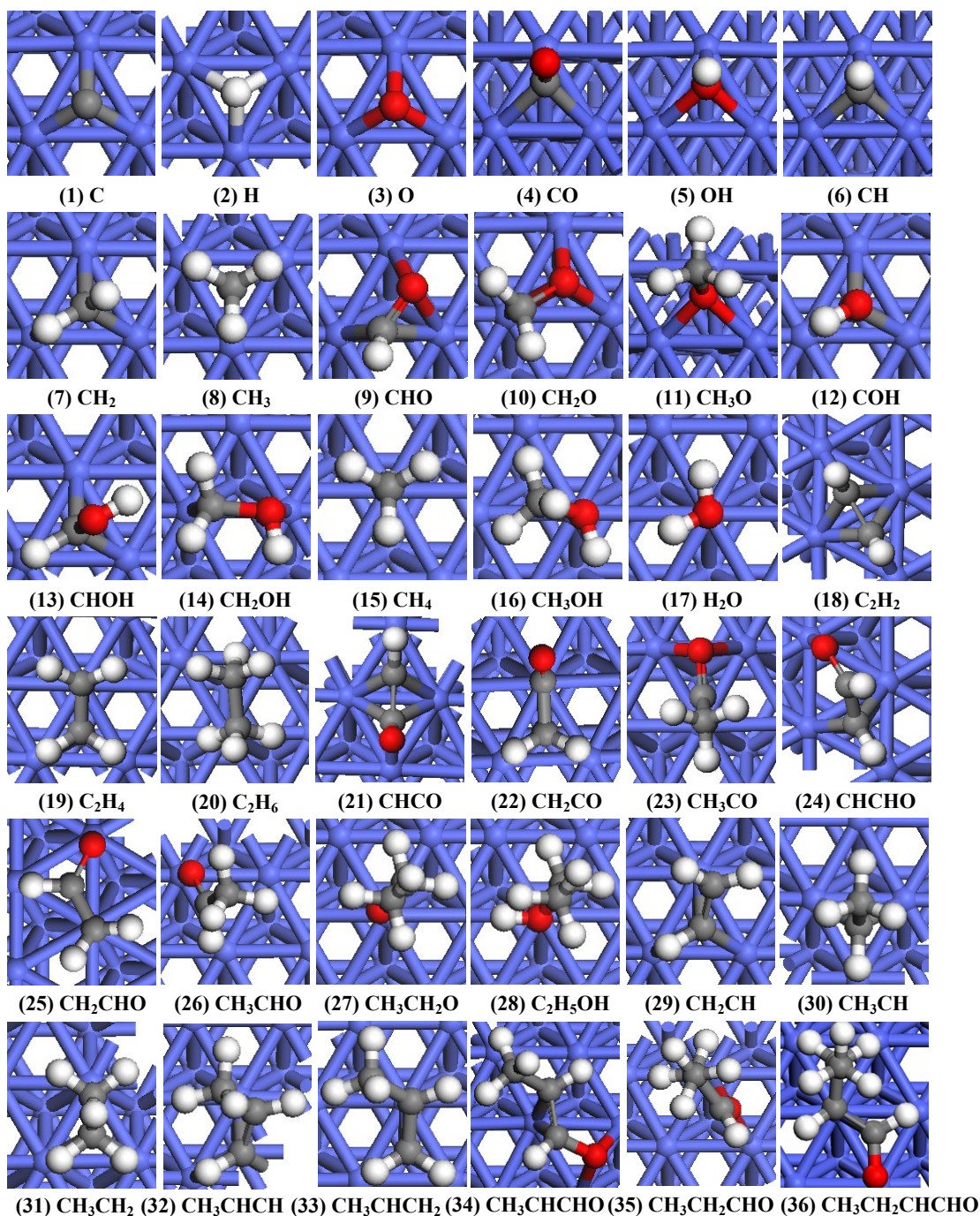


Figure S2 The most stable adsorption configurations of all possible species involved in syngas conversion on Co(0001) surface. The Co, C, H and O atoms are shown in the purple, grey, white and red balls, respectively. The energies are in $\text{kJ}\cdot\text{mol}^{-1}$.

CH₃CHCHO and CH₃CH₂CHO CH₃CHCHO prefers to adsorb at the fcc site with the bridge(O)-top(α -C and β -C) configuration, the adsorption free energy is $156.5 \text{ kJ}\cdot\text{mol}^{-1}$. CH₃CH₂CHO prefers to adsorb at the bridge site with the C–O bond nearly perpendicular to the surface, the corresponding adsorption free energy is only $-5.4 \text{ kJ}\cdot\text{mol}^{-1}$.

CH₃CH₂CHCHO CH₃CH₂CHCHO prefers to adsorb at the fcc site with the bridge(O)-top(α -C and β -C) configuration, the adsorption free energy is 178.9 kJ·mol⁻¹.

Part 4. CH_x($x=1\sim 3$) and CH₃OH Formation from Syngas

Starting from CO activation, all possible elementary reactions, the corresponding activation (free) energy (ΔG_a , kJ·mol⁻¹), reaction energies (ΔG , kJ·mol⁻¹) and the reaction rate constant (k , s⁻¹ or L·mol⁻¹·s⁻¹) at 500 K, as well as the only one imaginary frequency of the transition state (ν_i , cm⁻¹) involving in syngas conversion on Co(0001) surface have been listed in [Table 1](#) in the main text.

Starting from CHO, CH_x($x=1\sim 3$) formations with or without H-assisted have been discussed, respectively. With respect to CHO and CHO+H, the potential energy profiles of CH_x($x=1\sim 3$) formation together with the structures of the initial states (ISs), transition states (TSs) and final states (FSs) at the temperature of 500 K are shown in [Figures S3~S5](#), respectively.

4.1 CH Formation

As displayed in [Figure S3](#), in R2-1, starting from CHO+H, CHO hydrogenation to CHOH via TS2-1 is endothermic by 29.1 kJ·mol⁻¹ with an activation free energy of 103.2 kJ·mol⁻¹, the rate constant is 7.00×10^3 L·mol⁻¹·s⁻¹.

For CH formation without H-assisted, in R2-2, CHO dissociates into CH+O via TS2-2, this reaction has an activation free energy of 68.9 kJ·mol⁻¹, and it is exothermic by 62.9 kJ·mol⁻¹. In R2-3, the C–O bond cleavage of CHOH goes through the transition state TS2-3 to produce CH+OH, this reaction is exothermic by 69.0 kJ·mol⁻¹ with an activation free energy of 78.8 kJ·mol⁻¹. These two elementary reactions have the rate constants of 2.33×10^6 and 9.91×10^4 s⁻¹, respectively.

For CH formation with H-assisted, in R2-4, the C–O bond scission of CHO with H-assisted leads to CH+OH via TS2-4, this elementary reaction is exothermic by 39.9 kJ·mol⁻¹ with an activation free energy of 82.8 kJ·mol⁻¹ and the rate constant of 2.42×10^4 L·mol⁻¹·s⁻¹. In R2-5, starting

from CHO+H, CHOH dissociation with H-assisted leads to CH+H₂O via TS2-5; in the final state, CH+H₂O, CH adsorbs at the hcp site, while H₂O is far away from the surface with its molecular plane nearly parallel to the surface; this reaction has an activation free energy of 60.3 kJ·mol⁻¹ with the corresponding rate constant $5.42 \times 10^6 \text{ L} \cdot \text{mol}^{-1} \cdot \text{s}^{-1}$, and it is exothermic by 19.6 kJ·mol⁻¹.

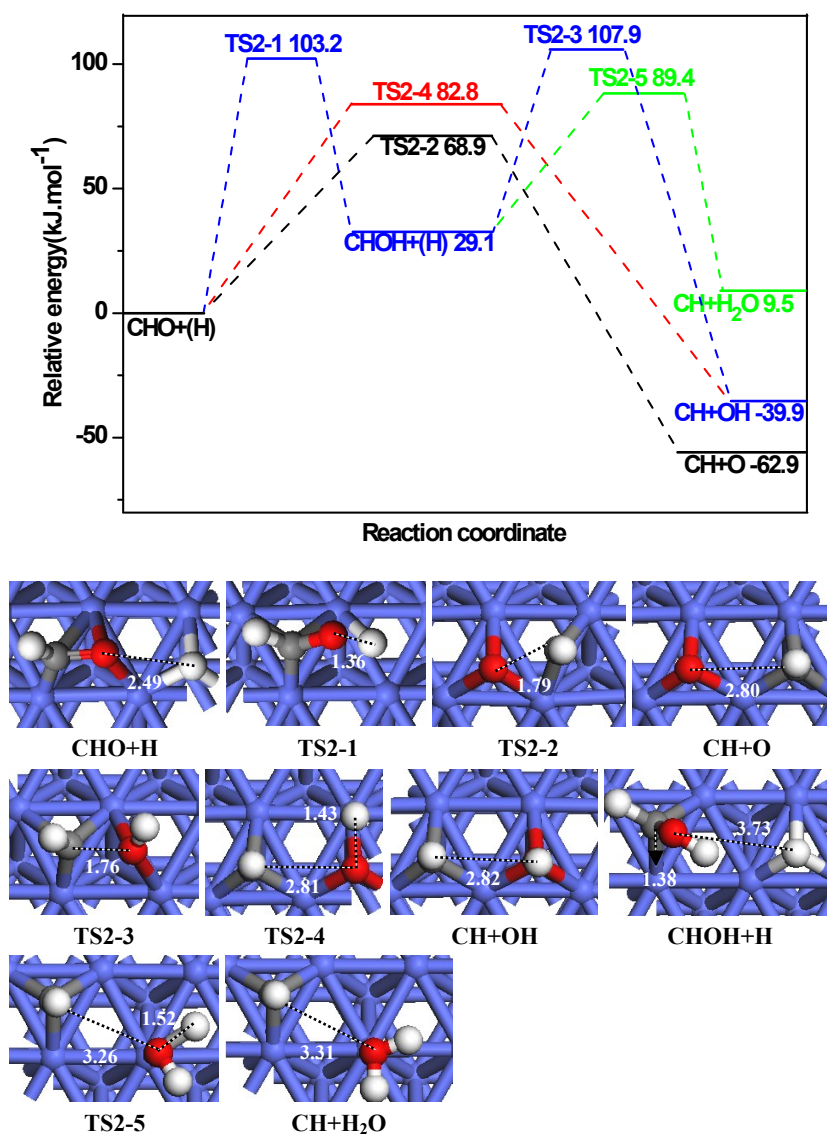


Figure S3 The potential energy profile of CH formation at 500 K with respect to CHO+H together with the structures of initial states (ISs), transition states (TSs) and final states (FSs); other structures are shown in Figure 2 in the main text. Bond lengths are in Å.

4.2 CH₂ Formation

As shown in Figure S4, the formations of CH₂O and CH₂OH are firstly investigated. In R3-1,

starting from CHO+H, the co-adsorbed CHO and H species goes through TS3-1 to form CH₂O, this reaction has an activation free energy of 47.4 kJ·mol⁻¹, and it is endothermic by 21.9 kJ·mol⁻¹. In R3-2, starting from CH₂O+H, the adsorbed CH₂O with H species goes through TS3-2 to form CH₂OH, this reaction is endothermic by 37.0 kJ·mol⁻¹ with an activation free energy of 115.7 kJ·mol⁻¹. In R3-3, the adsorbed H atom approaches to CHOH to form CH₂OH via TS3-3, this reaction has an activation free energy of 66.0 kJ·mol⁻¹, and it is endothermic by 29.8 kJ·mol⁻¹. The rate constants of above three reactions are 2.50×10^8 , 4.41×10^1 and $4.90 \times 10^6 \text{ L} \cdot \text{mol}^{-1} \cdot \text{s}^{-1}$, respectively.

For CH₂ formation without H-assisted, in R3-4, CH₂O dissociates into CH₂+O via TS3-4, this elementary reaction is exothermic by 59.6 kJ·mol⁻¹, and it has an activation free energy of 97.2 kJ·mol⁻¹ with the rate constant of $3.01 \times 10^3 \text{ s}^{-1}$. In R3-5, the direct C–O bond cleavage of CH₂OH to CH₂+OH via TS3-5 is exothermic by 79.8 kJ·mol⁻¹ with an activation free energy of 38.1 kJ·mol⁻¹, and the corresponding rate constant is $1.70 \times 10^9 \text{ s}^{-1}$.

For CH₂ formation with H-assisted, in R3-6, the TS obtained for CHO dissociation with H-assisted to CH₂+O is similar to that of CHO hydrogenation to CH₂O, suggesting that CHO with H-assisted prefers to be hydrogenated to CH₂O rather than being dissociated into CH₂+O. In R3-7, the C–O bond cleavage of CH₂O with H-assisted produces CH₂+OH via TS3-7, this reaction is exothermic by 42.8 kJ·mol⁻¹ with an activation free energy of 63.0 kJ·mol⁻¹. In R3-8, the TS obtained for CHOH dissociation with H-assisted to produce CH₂+OH is similar to that of CHOH hydrogenation to CH₂OH, indicating that CHOH with H-assisted prefers to be hydrogenated to CH₂OH rather than being dissociated into CH₂+OH. In R3-9, CH₂OH dissociation with H-assisted to CH₂+H₂O via TS3-9 has an activation free energy of 26.2 kJ·mol⁻¹, and it is exothermic by 52.0 kJ·mol⁻¹. The reaction rate constants of R3-7 and R3-9 are 2.63×10^6 and $6.21 \times 10^{10} \text{ L} \cdot \text{mol}^{-1} \cdot \text{s}^{-1}$, respectively.

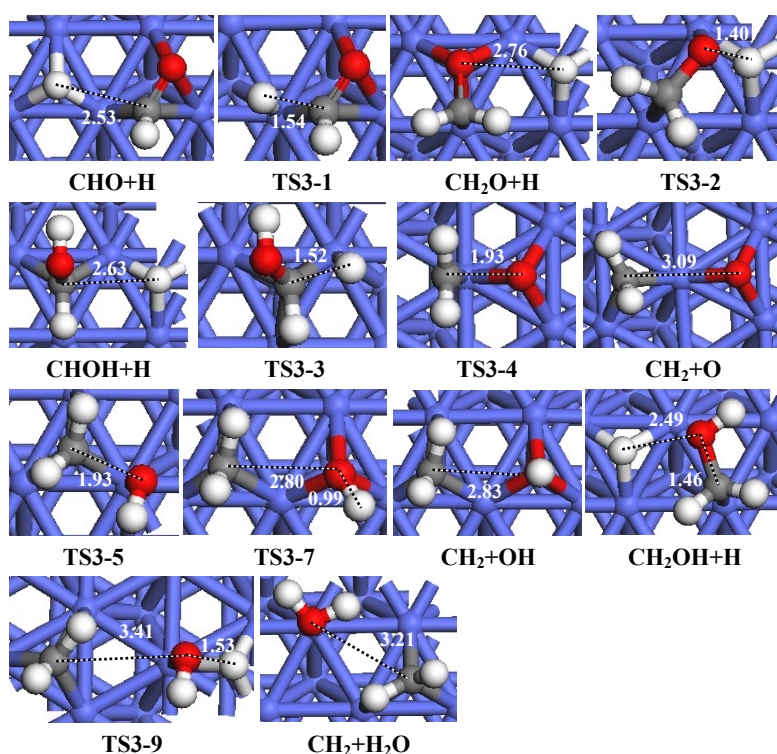
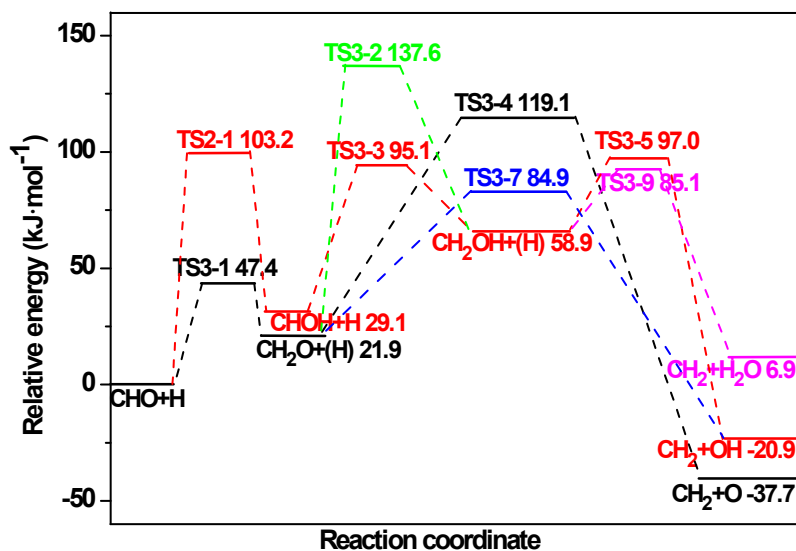


Figure S4 The potential energy profile of CH_2 formation at 500 K with respect to $\text{CHO}+\text{H}$ together with the structures of ISs, TSs and FSs ; other structures are shown in Figure S2 in the main text. Bond lengths are in Å.

4.3 CH_3 Formation

As presented in Figure S5, the formations of CH_3O and CH_3OH have three possible reactions (R4-1~R4-3). In R4-1, H atom approaches to C atom of CH_2O to produce CH_3O via TS4-1. In R4-2, CH_3O hydrogenates to CH_3OH via TS4-2. In R4-3, CH_2OH hydrogenates to CH_3OH via TS4-3.

The activation free energies of these three reactions are 50.0, 137.3 and 78.3 kJ·mol⁻¹ with the corresponding reaction free energies of -26.7, 48.8 and -14.9 kJ·mol⁻¹, respectively; the corresponding reaction rate constants are 1.81×10^8 , 8.60×10^{-1} and 3.60×10^5 L·mol⁻¹·s⁻¹, respectively.

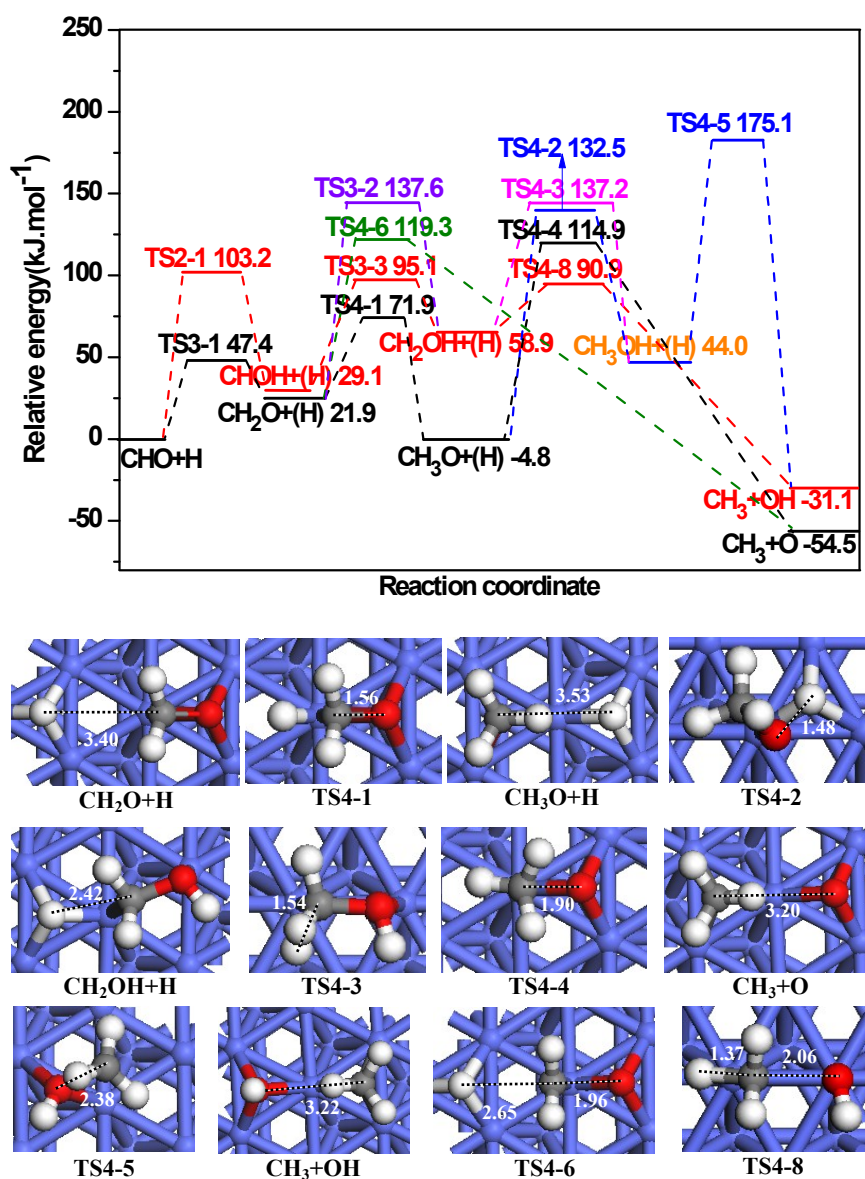


Figure S5 The potential energy profile of CH₃ formation at 500 K together with the structures of ISs, TSs and FSs with respect to CHO+H; other structures are shown in Figure S2 in the main text. Bond lengths are in Å.

For CH₃ formation without H-assisted, in R4-4 and R4-5, the direct dissociation of CH₃O and CH₃OH lead to CH₃ species via TS4-4 and TS4-5, respectively. Both reactions have the activation free energies of 119.7 and 131.1 kJ·mol⁻¹ with the reaction free energies of -49.7 and -75.1 kJ·mol⁻¹, respectively. The rate constants for these two reactions are 3.92×10^0 and 4.03×10^1 s⁻¹, respectively.

For CH_3 formation with H-assisted, in R4-6, the C–O bond scission of CH_2O with H-assisted produces CH_3+O via TS4-6, this reaction has an activation free energy of $97.4 \text{ kJ}\cdot\text{mol}^{-1}$ with the reaction free energy of $-76.4 \text{ kJ}\cdot\text{mol}^{-1}$, the corresponding reaction rate constant is $1.38\times 10^3 \text{ L}\cdot\text{mol}^{-1}\cdot\text{s}^{-1}$. In R4-7, the TS obtained for CH_3O dissociation with H-assisted to produce CH_3+OH is similar to that of CH_3O hydrogenation to CH_3OH , indicating that CH_3O with H-assisted prefers to be hydrogenated to CH_3OH rather than being dissociated into CH_3+OH . In R4-8, the C–O bond cleavage of CH_2OH with H-assisted goes through TS4-8 to form CH_3+OH , this reaction is exothermic by $90.0 \text{ kJ}\cdot\text{mol}^{-1}$, and it has an activation free energy of $32.0 \text{ kJ}\cdot\text{mol}^{-1}$ with the rate constant of $1.48\times 10^{10} \text{ L}\cdot\text{mol}^{-1}\cdot\text{s}^{-1}$.

4.4 CH_3OH Formation

As displayed in Figure S6, with respect to $\text{CHO}+\text{H}$, the pathways of $\text{CHO}+3\text{H}\rightarrow\text{CHOH}+2\text{H}\rightarrow\text{CH}_2\text{OH}+\text{H}\rightarrow\text{CH}_3\text{OH}$, $\text{CHO}+3\text{H}\rightarrow\text{CH}_2\text{O}+2\text{H}\rightarrow\text{CH}_2\text{OH}+\text{H}\rightarrow\text{CH}_3\text{OH}$ and $\text{CHO}+3\text{H}\rightarrow\text{CH}_2\text{O}+2\text{H}\rightarrow\text{CH}_3\text{O}+\text{H}\rightarrow\text{CH}_3\text{OH}$ have the close overall activation free energies of 137.2, 137.6 and 132.5 $\text{kJ}\cdot\text{mol}^{-1}$, respectively.

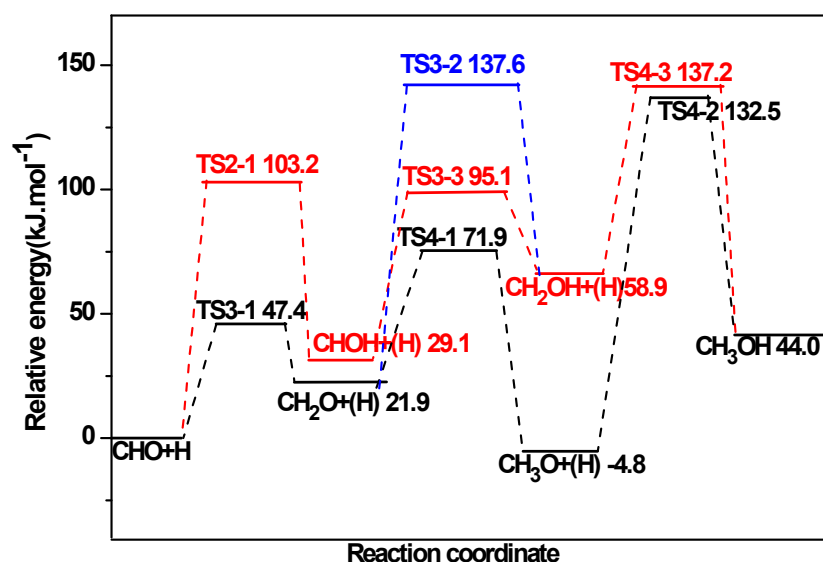


Figure S6 The potential energy profile of CH_3OH formation with respect to $\text{CHO}+\text{H}$ species at 500 K.

However, the rate constant of the rate-limiting step $\text{CHO}+\text{H}\rightarrow\text{CHOH}$ in the first pathway is $7.00\times 10^3 \text{ L}\cdot\text{mol}^{-1}\cdot\text{s}^{-1}$, $4.41\times 10^1 \text{ L}\cdot\text{mol}^{-1}\cdot\text{s}^{-1}$ of $\text{CH}_2\text{O}+\text{H}\rightarrow\text{CH}_2\text{OH}$ in the second pathway, $8.60\times 10^{-1} \text{ L}\cdot\text{mol}^{-1}\cdot\text{s}^{-1}$ of $\text{CH}_3\text{O}+\text{H}\rightarrow\text{CH}_3\text{OH}$ in the third pathway. Therefore, $\text{CHO}+3\text{H}\rightarrow\text{CHOH}+2\text{H}\rightarrow\text{H}_2\text{OH}+\text{H}\rightarrow\text{CH}_3\text{OH}$ is the most favorable pathway for CH_3OH formation.

Part 5. The Reactions Related to $\text{CH}_x(x=2,3)$ Species

The potential energy profile for the dissociation, hydrogenation and coupling of $\text{CH}_x(x=2,3)$, as well as CO/CHO insertion into $\text{CH}_x(x=2,3)$ is shown in [Figures S7](#) and [S8](#), respectively.

As shown in [Figure S7](#), for CH_2 dissociation into CH and H, this reaction is exothermic by $29.9 \text{ kJ}\cdot\text{mol}^{-1}$ with an activation free energy of $20.8 \text{ kJ}\cdot\text{mol}^{-1}$ and a rate constant of $2.52\times 10^{10} \text{ s}^{-1}$. CH_2 hydrogenation to CH_3 needs an activation free energy of $50.8 \text{ kJ}\cdot\text{mol}^{-1}$ with the rate constant of $1.15\times 10^8 \text{ L}\cdot\text{mol}^{-1}\cdot\text{s}^{-1}$, it is exothermic by $7.6 \text{ kJ}\cdot\text{mol}^{-1}$. For CH_2 coupling, this reaction is exothermic by $39.8 \text{ kJ}\cdot\text{mol}^{-1}$ with an activation free energy of $68.3 \text{ kJ}\cdot\text{mol}^{-1}$ and a rate constant of $1.71\times 10^6 \text{ L}\cdot\text{mol}^{-1}\cdot\text{s}^{-1}$. For CO insertion into CH_2 , this reaction is endothermic by $59.0 \text{ kJ}\cdot\text{mol}^{-1}$ with an activation free energy of $87.2 \text{ kJ}\cdot\text{mol}^{-1}$; while CHO insertion into CH_2 has a relative low activation free energy of $33.3 \text{ kJ}\cdot\text{mol}^{-1}$, and it is exothermic by $24.6 \text{ kJ}\cdot\text{mol}^{-1}$, the rate constants for these two insertion reactions are 2.46×10^4 and $6.96\times 10^9 \text{ L}\cdot\text{mol}^{-1}\cdot\text{s}^{-1}$, respectively. CH_2 coupling with CH has an activation free energy and a reaction free energy of 73.8 and $-7.1 \text{ kJ}\cdot\text{mol}^{-1}$, respectively, and the rate constant is $3.25\times 10^5 \text{ L}\cdot\text{mol}^{-1}\cdot\text{s}^{-1}$.

As shown in [Figure S8](#), for CH_3 dissociation into CH_2 and H, this elementary reaction is endothermic by $8.4 \text{ kJ}\cdot\text{mol}^{-1}$ with an activation free energy of $58.4 \text{ kJ}\cdot\text{mol}^{-1}$ and the rate constant of $1.17\times 10^7 \text{ s}^{-1}$. CH_3 hydrogenation to CH_4 has an activation free energy of $98.9 \text{ kJ}\cdot\text{mol}^{-1}$ with the reaction free energy of $2.6 \text{ kJ}\cdot\text{mol}^{-1}$, it has the rate constant of $3.99\times 10^3 \text{ L}\cdot\text{mol}^{-1}\cdot\text{s}^{-1}$. For CH_3 coupling, it is exothermic by $23.0 \text{ kJ}\cdot\text{mol}^{-1}$ with a large activation free energy of $150.4 \text{ kJ}\cdot\text{mol}^{-1}$ and

the rate constant of $6.18 \times 10^{-3} \text{ L} \cdot \text{mol}^{-1} \cdot \text{s}^{-1}$. CO insertion into CH_3 is endothermic by $59.0 \text{ kJ} \cdot \text{mol}^{-1}$ with an activation free energy of $141.7 \text{ kJ} \cdot \text{mol}^{-1}$ and a rate constant of $1.11 \times 10^{-1} \text{ L} \cdot \text{mol}^{-1} \cdot \text{s}^{-1}$. CHO insertion into CH_3 has an activation free energy of $100.5 \text{ kJ} \cdot \text{mol}^{-1}$ with the rate constant of $1.52 \times 10^3 \text{ L} \cdot \text{mol}^{-1} \cdot \text{s}^{-1}$, and it is endothermic by $12.4 \text{ kJ} \cdot \text{mol}^{-1}$.

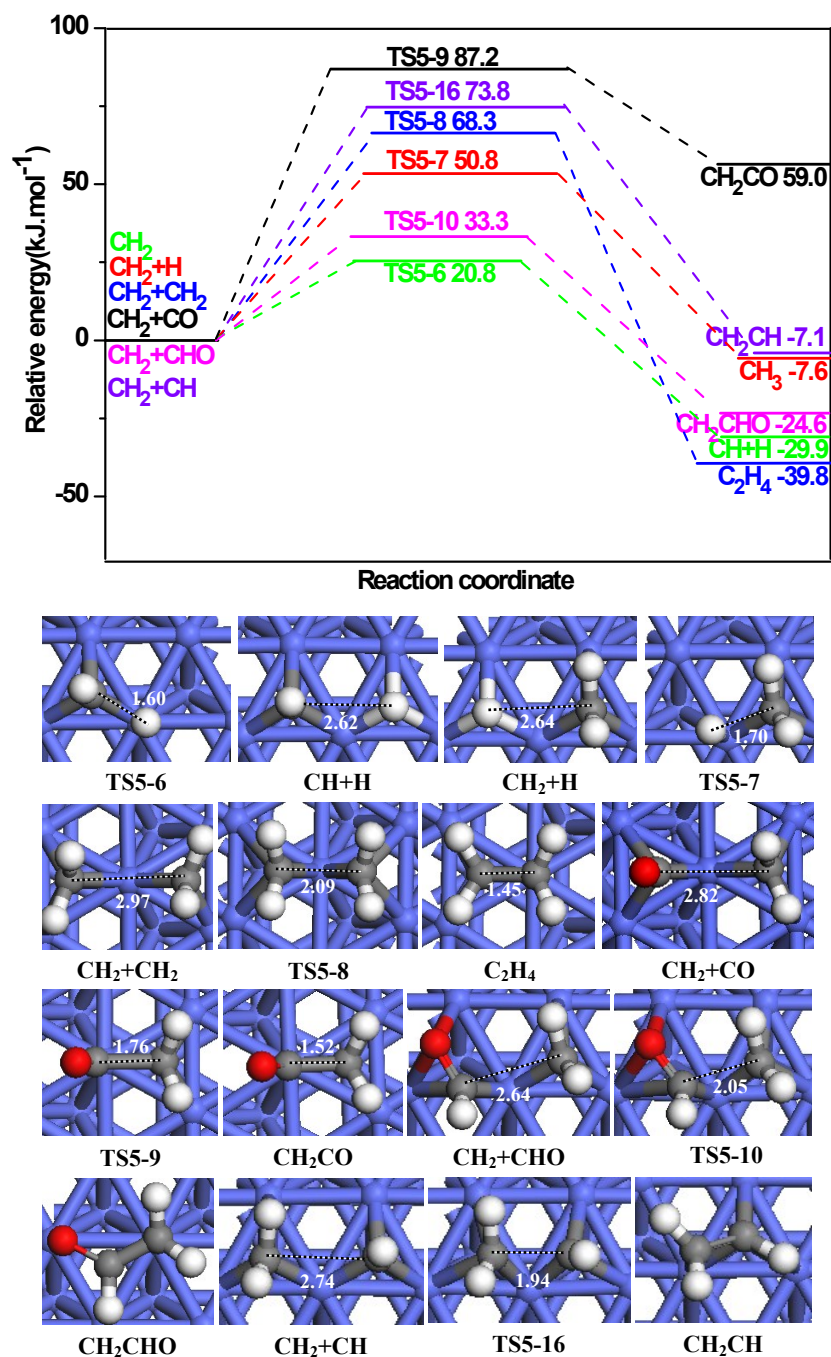


Figure S7 The potential energy profile of CH_2 dissociation, hydrogenation, coupling and CHO/CO insertion reactions at 500 K together with the structures of ISs, TSs and FSs; other structures are shown in Figure S2 in the main text. Bond lengths are in Å.

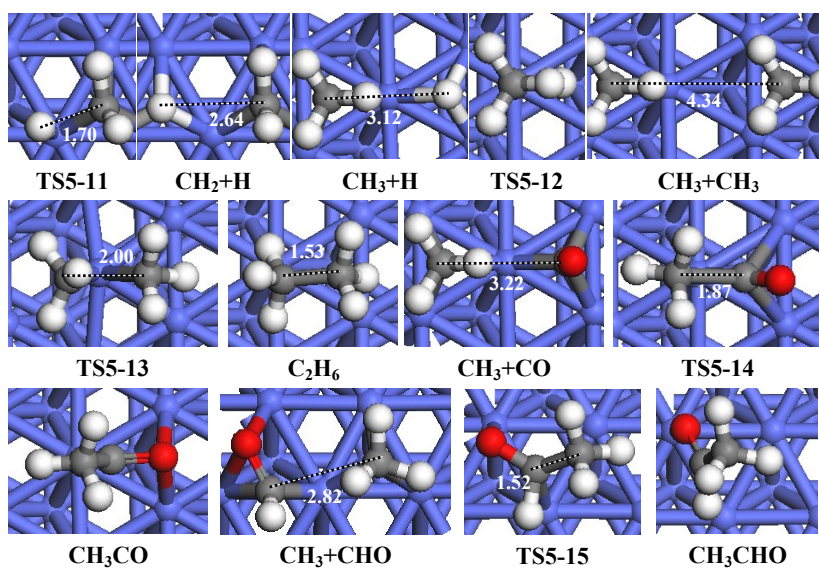
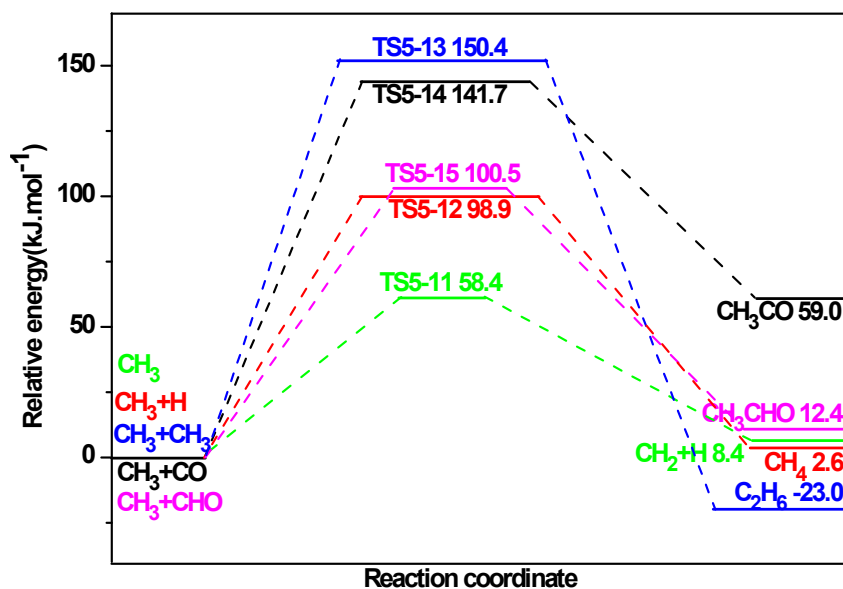


Figure S8 The potential energy profile of CH₃ dissociation, hydrogenation, coupling and CHO/CO insertion reactions at 500 K together with the structures of ISs, TSs and FSS; other structures are shown in Figure S2 in the main text. Bond lengths are in Å.

Part 6. The Reactions Related to CHCHO, CH₂CHO and CH₃CHO Intermediates

The potential energy profile related to CH_xCHO (x=1~3) intermediates at 500 K together with the structures of ISs, TSs and FSS can be seen in Figure S9.

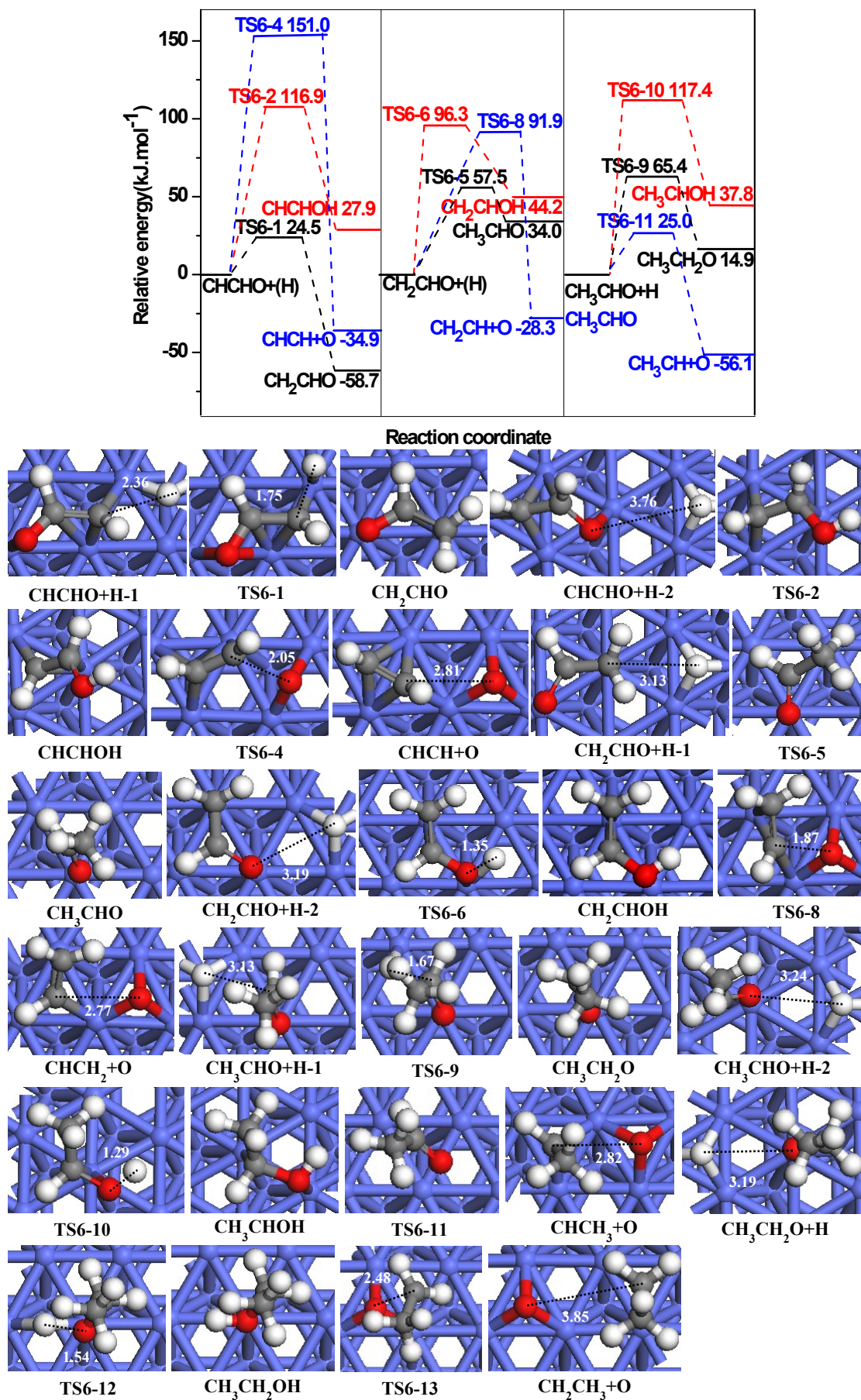


Figure S9 The potential energy profile of the reactions related to CH_xCHO ($x=1\sim 3$) intermediates at 500 K together with the structures of ISs, TSs and FSs involved in C_2 oxygenates formation. Bond lengths are in Å.

Starting from CHCHO intermediate, in R6-1, CHCHO hydrogenation to CH₂CHO has only an activation free energy of 24.5 kJ·mol⁻¹, it is exothermic by 58.7 kJ·mol⁻¹. In R6-2, CHCHO hydrogenation to CHCHOH has an activation free energy of 116.9 kJ·mol⁻¹, it is endothermic by 27.9 kJ·mol⁻¹. However, in R6-3, our results show that CHCH₂O intermediate cannot stably exist, suggesting that there will be no CHCH₂O intermediate under the realistic conditions. In R6-4, CHCHO dissociation into CHCH and O needs an activation free energy of 151.0 kJ·mol⁻¹, and it is exothermic by 34.9 kJ·mol⁻¹. The corresponding reaction rate constants of R6-1, R6-2 and R6-4 are 7.53×10^{10} , $2.35 \times 10^1 \text{ L} \cdot \text{mol}^{-1} \cdot \text{s}^{-1}$ and $1.16 \times 10^{-2} \text{ s}^{-1}$, respectively. Thus, with CHCHO hydrogenation to CH₂CHO (R6-1) is the most favorable among all reactions related to CHCHO intermediate.

Starting from CH₂CHO intermediate, in R6-5, CH₂CHO hydrogenation to CH₃CHO has an activation free energy of 57.5 kJ·mol⁻¹, it is endothermic by 34.0 kJ·mol⁻¹. In R6-6, CH₂CHO hydrogenation to CH₂CHOH is endothermic by 44.2 kJ·mol⁻¹ with an activation free energy of 96.3 kJ·mol⁻¹. However, in R6-7, our results show that CH₂CH₂O intermediate cannot stably exist under the realistic condition. In R6-8, CH₂CHO dissociation into CH₂CH and O needs to overcome an activation free energy of 91.9 kJ·mol⁻¹, it is exothermic by 28.3 kJ·mol⁻¹. The reaction rate constants of R6-5, R6-6 and R6-8 these three reactions are 1.41×10^8 , $3.53 \times 10^3 \text{ L} \cdot \text{mol}^{-1} \cdot \text{s}^{-1}$ and $2.35 \times 10^3 \text{ s}^{-1}$, respectively. Thus, CH₂CHO prefers to be hydrogenated to CH₃CHO among the all mentioned reactions related to CH₂CHO intermediate.

Starting from CH₃CHO intermediate, CH₃CHO hydrogenation to CH₃CH₂O in R6-9 is endothermic by 14.9 kJ·mol⁻¹, it has an activation free energy of 65.4 kJ·mol⁻¹ and a reaction rate constant of $2.40 \times 10^7 \text{ L} \cdot \text{mol}^{-1} \cdot \text{s}^{-1}$. In R6-10, CH₃CHO hydrogenation to CH₃CHOH has an activation free energy of 117.4 kJ·mol⁻¹ with the rate constant of $6.30 \times 10^0 \text{ L} \cdot \text{mol}^{-1} \cdot \text{s}^{-1}$, and it is endothermic by 37.8 kJ·mol⁻¹. However, in R6-11, CH₃CHO dissociation into CH₃CH and O only needs an

activation free energy of $25.0 \text{ kJ}\cdot\text{mol}^{-1}$, and possess the largest reaction rate constant of $3.77\times 10^{11} \text{ s}^{-1}$. Meanwhile, CH_3CHO dissociation into CH_3CH is more favorable than its hydrogenation. As a result, among all mentioned reactions related to CH_3CHO intermediate, CH_3CH prefers to be formed through the C–O bond cleavage of CH_3CHO dissociation.

Part 7. The Structures of ISs, TSs and FSs for the Chain Growth Starting from CH_3CHCHO

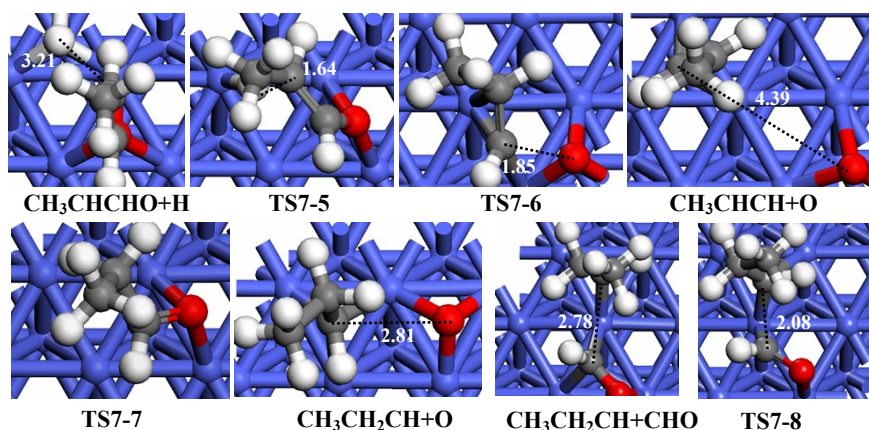


Figure S10 The structures of ISs, TSs and FSs for the chain growth reactions starting from CH_3CHCHO ; other structures are shown in [Figure S2](#) in the main text. Bond lengths are in Å.

References

- [1] X. C. Fu, W. X. Shen, T. Y. Yao, *Physical Chemistry*, Higher Education 4th edn, 1990.
- [2] Y. A. Zhu, D. Chen, X. G. Zhou, W. K. Yuan, *Catal. Today*, 2009, **148**, 260–267.
- [3] X. M. Cao, R. Burch, C. Hardacre, P. Hu, *Catal. Today*, 2011, **165**, 71–79.
- [4] X. M. Cao, R. Burch, C. Hardacre, P. Hu, *J. Phys. Chem. C*, 2011, **115**, 19819–19827.
- [5] X. Q. Gong, R. Raval, P. Hu, *Surf. Sci.*, 2004, **562**, 247–256.
- [6] L. Joos, I. A. W. Filot, S. Cottenier, E. J. M. Hensen, M. Waroquier, V. V. Speybroeck, R. A. van Santen, *J. Phys. Chem. C*, 2014, **118**, 5317–5327.
- [7] Q. Ge, M. Neurock, H. A. Wright, N. Srinivasan, *J. Phys. Chem. B*, 2002, **106**, 2826–2829.
- [8] J. Cheng, P. Hu, P. Ellis, S. French, G. Kelly, C. Martin Lok, *J. Phys. Chem. C*, 2008, **112**, 9464–9473.